

Molecular Orbital Studies of Hydrogen Bonds. V. Analysis of the Hydrogen-Bond Energy between Lower Excited States of H₂CO and H₂O

Suehiro Iwata and Keiji Morokuma*

Contribution from the Department of Chemistry, University of Rochester,
Rochester, New York 14627. Received June 6, 1973

Abstract: *Ab initio* calculations for the interacting system of lower excited states of planar and bent H₂CO with H₂O are carried out using the recently proposed electron-hole potential method. The hydrogen-bond energy in each state is decomposed into the electrostatic, exchange-repulsion, polarization-resonance, and charge-transfer contributions in order to find the origin of the hydrogen bonding. The effects of the basis sets on the excited state hydrogen-bond energy and its decomposition are also examined. The hydrogen bond energy and its components are rather sensitive to the basis sets. Despite this dependency, within each basis set the general characteristics of the hydrogen bonding of various states are reasonably well described by energy components. In addition, the hydrogen-bond energy of the trimer H₂CO-2H₂O is related to the observed shift of electronic transitions.

Ab initio SCF-MO methods have been successfully used for study of the hydrogen bonding between the ground state molecules,¹⁻³ including H₂CO-H₂O.¹ In the previous letter,⁴ we reported the first *ab initio* hydrogen-bond calculations between the lower excited states of formaldehyde (H₂CO) and a water molecule. In the present paper for the same system, we analyze the hydrogen-bond energy of each state in terms of components (the electrostatic, exchange-repulsion, polarization-resonance, and charge-transfer energies) and discuss the correlation of contributions with the population analysis. The determining factors of the hydrogen-bonding formation would be made clear by the comparison of the decomposition between the different states and between the different geometries.

It is well known experimentally that the $n-\pi^*$ transition generally shows a large blue shift upon hydrogen bonding while the $\pi-\pi^*$ transition in conjugated molecules makes a small red shift.⁵ This criterion is further used experimentally to distinguish $\pi-\pi^*$ transitions.⁵ Also, the photochemical behavior and emission spectra of carbonyl compounds in solution have been extensively studied experimentally.⁶ Formaldehyde is the simplest carbonyl compound which has both $n-\pi^*$ and $\pi-\pi^*$ excited states. We felt therefore that the H₂CO-H₂O system would serve well as a model for general theoretical studies of the hydrogen bonding in the excited carbonyl compounds.

In the present paper, we use the electron-hole potential method (EHP) which we proposed recently⁷ to calculate the wave function and energy of excited states. Geometries and basis functions used will be mentioned in section IA, and in section IB features of the EHP method are discussed briefly. In section IC

the scheme of the decomposition of the hydrogen bond energy is presented. In section IIA we compare the EHP results with the configuration interaction (CI) results for excited states of the formaldehyde monomer. The energy decomposition for the ground and lower excited states in the various geometries is given in sections IIB-D. Excited states of the trimer H₂CO ··· 2H₂O will be considered in section IIE. Since the carbonyl group can form two hydrogen bonds in the solution,¹ this would be a more realistic model for comparison with experiments. In section III the effect of various basis sets (STO-3G and 4-31G with or without additional diffuse p orbitals) on the hydrogen-bond energy and its decomposition will be discussed.

I. Methods

A. Basis Functions and Geometry. A minimal Slater basis set was used in most calculations with the POLYCAL integral and SCF program.⁸ The orbital exponents and geometry were optimized for the ground state of each molecule, which were summarized in our previous paper.¹ In section III contracted Gaussian STO-3G and 4-31G basis sets with or without a set of extra diffuse p orbitals were used with the GAUSSIAN 70 program.⁹ The STO-3G scale factors are those recommended by Hehre, Stewart, and Pople¹⁰ and the 4-31G scale factors are by Ditchfield, Hehre, and Pople.¹¹

In addition to the planar H₂CO geometry, calculations were carried out for the bent H₂CO. The experimental geometry for the $n-\pi^*$ singlet state ($R(\text{C}=\text{O}) = 1.323 \text{ \AA}$, $R(\text{C}-\text{H}) = 1.093 \text{ \AA}$, $\angle(\text{HCH}) = 119^\circ$, and the out-of-plane angle = 31°)¹² was assumed throughout. The experimental $n-\pi^*$ triplet geometry is very similar to the singlet one. Although the geometries of other higher excited states are not known experimentally,

(1) K. Morokuma, *J. Chem. Phys.*, **55**, 1236 (1971).

(2) K. Morokuma and L. Pedersen, *J. Chem. Phys.*, **48**, 3275 (1968); K. Morokuma and J. R. Winick, *ibid.*, **52**, 1301 (1970).

(3) P. A. Kollman and L. C. Allen, *Chem. Rev.*, **72**, 283 (1972), and references therein.

(4) S. Iwata and K. Morokuma, *Chem. Phys. Lett.*, **19**, 94 (1973), part IV of this series.

(5) G. C. Pimentel and A. L. McClellan, "The Hydrogen Bond," W. H. Freeman, San Francisco, Calif., 1960.

(6) J. G. Calvert and J. N. Pitts, Jr., "Photochemistry," Wiley, New York, N. Y., 1966.

(7) K. Morokuma and S. Iwata, *Chem. Phys. Lett.*, **16**, 192 (1972).

(8) R. M. Stevens, *J. Chem. Phys.*, **52**, 1397 (1970).

(9) W. J. Hehre, W. A. Lathan, R. Ditchfield, M. D. Newton, and J. A. Pople, submitted to Quantum Chemistry Program Exchange, Indiana University.

(10) W. J. Hehre, R. F. Stewart, and J. A. Pople, *J. Chem. Phys.*, **51**, 2657 (1969).

(11) R. Ditchfield, W. J. Hehre, and J. A. Pople, *J. Chem. Phys.*, **54**, 724 (1971).

(12) G. Herzberg, "Electronic Spectra, Polyatomic Molecules," Van Nostrand, Princeton, N. J., 1966.

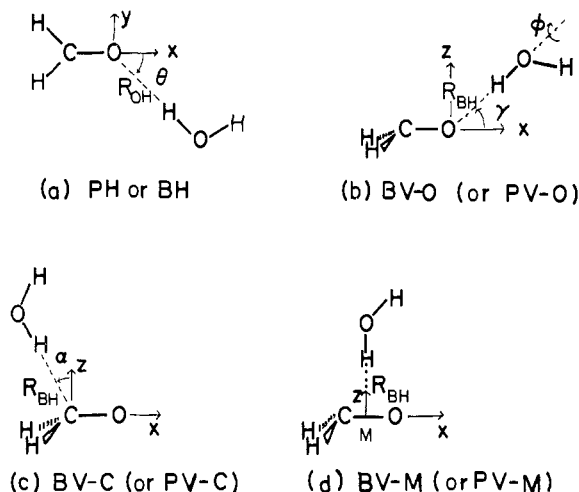


Figure 1. Models of hydrogen-bond complex between H_2CO and H_2O . The first letter P and B indicate planar and bent H_2CO , respectively. The second letter H stands for horizontal and V for vertical. The third letter, O, C, and M, specifies the point of approach as O atom, C atom, and the midpoint of the bond, respectively.

theoretical calculations suggest a bent structure for the $\pi-\pi^*$ triplet and singlet states.¹³⁻¹⁵

In the interacting system the monomer geometries are assumed to be maintained. Various model structures of the hydrogen-bonding system used in the calculation are shown in Figure 1. The C-O bond of formaldehyde is fixed on the x axis. The (xz) plane is a bisector of the HCH angle and is a mirror plane of formaldehyde. In the planar model a formaldehyde molecule lies in the (xy) plane. In the model of Figure 1a, the water molecule also lies in the (xy) plane and $\text{O}-\text{H}\cdots\text{O}$ is collinear. We call the geometry of Figure 1a PH (for planar H_2CO , horizontal approach) and BH (for bent H_2CO , horizontal approach). The PH model has been found to be the most stable for the ground state.¹ Variations of two geometrical parameters R_{OH} and θ , as defined in the figure, are examined for both PH and BH models. In Figures 1b-d, the water molecule approaches H_2CO within the (xz) plane (the vertical approach). In Figure 1b, the HO bond is collinear with the formaldehyde O. The model is called PV-O (for planar H_2CO , vertical, and to oxygen) and BV-O (for bent H_2CO , vertical, and to oxygen). The geometry parameters to be changed are the $\text{O}\cdots\text{H}$ distance R_{BH} , the angle γ , and the rotation angle ϕ of H_2O around the $\text{O}-\text{H}\cdots\text{O}$ axis, where $\phi = 0$ when the nonbonding H of water is trans against $\text{O}-\text{C}$ with respect to $\text{O}-\text{H}\cdots\text{O}$. In Figure 1c, the HO bond approaches collinearly the formaldehyde C. Two parameters, the $\text{C}\cdots\text{H}$ distance R_{BH} and the angle α , are changed. The nonbonding OH of H_2O is assumed cis against CO with respect to $\text{O}-\text{H}\cdots\text{C}$. The model is called PV-C and BV-C. In Figure 1d, the HO approaches collinearly the midpoint M of the C-O bond. Furthermore, it is assumed that the approach is perpendicular to the C-O bond and that the bonding OH is cis against MO with respect to $\text{O}-\text{H}\cdots\text{M}$. The

$\text{M}\cdots\text{H}$ distance R_{BH} is varied. The model is called PV-M and BV-M.

Actual calculations were performed for 26 planar H_2CO and 24 bent H_2CO models, respectively.

B. The Electron-Hole Potential Method. The electron-hole potential method (EHP) or extended Hartree-Fock method for excited states which we recently proposed^{7,16} was used to calculate the wave function and the energy of the excited states of the hydrogen-bonded system. In EHP the wave function of an excited state is described by a one-electron excited configuration, say an excitation from the molecular orbital (MO) ϕ_α to ϕ_μ . The MO ϕ_α is expanded within the occupied orbital space $\{\psi_j\}$ of the ground state SCF-MO's as

$$\phi_\alpha = \sum_j^{\text{occ}} a_{\alpha j} \psi_j \quad (1)$$

and the orbital ϕ_μ is expanded within the vacant orbital space $\{\psi_k\}$ of the ground state SCF-MO's as

$$\phi_\mu = \sum_k^{\text{vac}} b_{\mu k} \psi_k \quad (2)$$

The coefficients $a_{\alpha j}$ and $b_{\mu k}$ are determined by the variational method, so that the excitation energy $\Delta E(\phi_\alpha \rightarrow \phi_\mu)$ is minimized.

The optimized MO's ϕ_α and ϕ_μ are obtained directly by solving the simultaneous pseudoeigenvalue problems iteratively.

$$\{F + P^\dagger(J_\mu - K_\mu \mp K_\mu)P\} \phi_\alpha = \lambda_\alpha \phi_\alpha \quad (3)$$

$$\{F + (1 - P^\dagger)(-J_\alpha + K_\alpha \pm K_\alpha) \times (1 - P)\} \phi_\mu = \lambda_\mu \phi_\mu \quad (4)$$

where F is the standard Hartree-Fock operator of the ground state and P is the projection operator onto the occupied orbital space

$$P = \sum_j^{\text{occ}} |\psi_j\rangle \langle \psi_j| \quad (5)$$

The operators J_μ and K_μ denote, as usual

$$J_\mu \phi_\alpha(1) = \int \phi_\mu^*(2) \phi_\mu(2) (1/r_{12}) \phi_\alpha(1) d\tau_2$$

$$K_\mu \phi_\alpha(1) = \int \phi_\mu^*(2) \phi_\alpha(2) (1/r_{12}) \phi_\mu(1) d\tau_2$$

and the upper and lower signs in eq 3 and 4 correspond to the singlet and triplet states, respectively.

Physically eq 3 and 4 mean that the wave function of the α hole feeling the potential field of the μ electron is determined within the occupied orbital space of the ground state SCF-MO, while the wave function of the μ electron moving in the field of the α hole is determined within the vacant orbital space. Therefore, the method can be called the electron-hole potential method.

The wave function of the $\phi_\alpha \rightarrow \phi_\mu$ state is expressed by a configuration using the new EHP-MO's $\{\phi\}$ as

$$\Phi(\alpha \rightarrow \mu) = 1/\sqrt{2} \{ |\phi_1 \bar{\phi}_1 \dots \phi_\alpha \bar{\phi}_\mu \dots \phi_n \bar{\phi}_n| \pm |\phi_1 \bar{\phi}_1 \dots \phi_\mu \bar{\phi}_\alpha \dots \phi_n \bar{\phi}_n| \} \quad (6)$$

where $| \dots |$ denotes a normalized Slater determinant. This function $\Phi(\alpha \rightarrow \mu)$ can be expanded in terms of a

(16) E. R. Davidson, *J. Chem. Phys.*, **57**, 1999 (1972).

(13) R. J. Buenker and D. S. Peyerimhoff, *J. Chem. Phys.*, **53**, 1368 (1970).

(14) K. Morokuma and J. H. Wu, unpublished work.

(15) R. Ditchfield, J. E. Del Bene, and J. A. Pople, *J. Amer. Chem. Soc.*, **94**, 4806 (1972).

linear combination of the one-electron excited configurations based on the canonical SCF-MO of the ground state as

$$\Phi(\alpha \rightarrow \mu) = \sum_j^{\text{occ}} \sum_k^{\text{vac}} a_{\alpha j} b_{\mu k} \psi_j \rightarrow \psi_k \quad (7)$$

We can compare the EHP with the configuration interaction (CI) including only one-electron excitation in which the wave function of the excited state is written as

$$\Phi = \sum_j^{\text{occ}} \sum_k^{\text{vac}} C_{jk} \psi_j \rightarrow \psi_k \quad (8)$$

The comparison of eq 7 and 8 reveals that the variation parameters in CI, C_{jk} , are decoupled into a product $a_{\alpha j} b_{\mu k}$ of new sets of coefficients $a_{\alpha j}$ and $b_{\mu k}$ which are variational parameters in the EHP method.

A few important advantages of the EHP method should be mentioned. The excited state wave function is expressed by a single electron configuration, eq 6, rather than a linear combination of configurations. Therefore, as well as in the SCF ground state, one can take full advantage of the orbital pictures in excited states in calculating expectation values of operators and in carrying out population analysis. The method is also well defined, simple, and systematic. Different from the CI, it does not include any correlation energy in the excited states, so the energy is more directly comparable with the SCF energy of the ground state.

A major improvement of the EHP method over the use of the ground state SCF occupied and virtual orbitals in calculating the excited state is illustrated by the following example and another example given before.⁴ For the H₂CO-H₂O hydrogen-bonded system in the BV-C geometry with $R_{\text{BH}} = 1.9 \text{ \AA}$ and $\gamma = 15^\circ$, the highest occupied MO ψ_{13} and the lowest vacant MO ψ_{14} of the ground state SCF calculation are given as

$$\psi_{13} = \{0.2732(\text{H}_1^{\text{F}} - \text{H}_2^{\text{F}}) - 0.7999(\text{O}_y^{\text{F}}) + 0.1531(\text{C}_y^{\text{F}})\} - 0.4685(\text{O}_y^{\text{W}})$$

$$\psi_{14} = \{0.1408(\text{H}_1^{\text{F}} + \text{H}_2^{\text{F}}) - 0.0002(\text{O}_{1s}^{\text{F}}) - 0.0102(\text{O}_{2s}^{\text{F}}) - 0.0588(\text{O}_x^{\text{F}}) + 0.7481(\text{O}_z^{\text{F}}) + 0.0458(\text{C}_{1s}^{\text{F}}) - 0.2485(\text{C}_{2s}^{\text{F}}) + 0.1586(\text{C}_z^{\text{F}}) - 0.6757(\text{C}_z^{\text{F}})\} + \{-0.1237(\text{H}_1^{\text{W}}) - 0.0339(\text{H}_2^{\text{W}}) - 0.0155(\text{O}_{1s}^{\text{W}}) + 0.1007(\text{O}_{2s}^{\text{W}}) + 0.0829(\text{O}_x^{\text{W}}) - 0.2044(\text{O}_z^{\text{W}})\}$$

where, for instance, O_y^{F} is the oxygen p_y orbital of formaldehyde, and H_1^{W} is the 1s orbital of the bonding hydrogen of water. The transition $\psi_{13} \rightarrow \psi_{14}$ is supposed to describe the lowest excitation in the complex. Both MO's are delocalized throughout the complex and cannot be easily assigned to H₂O or H₂CO. After completing the EHP procedure for the triplet state corresponding to this transition $13 \rightarrow 14$, one obtains the following new MO's.

$$\phi_{13} = \{0.2288(\text{H}_1^{\text{F}} - \text{H}_2^{\text{F}}) - 0.9693(\text{O}_y^{\text{F}}) + 0.0556(\text{C}_y^{\text{F}})\} - 0.0039(\text{O}_y^{\text{W}})$$

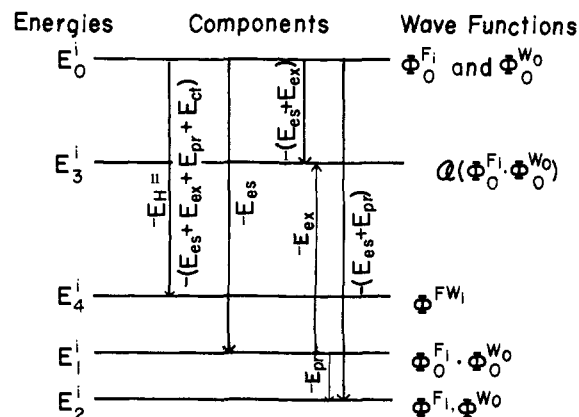


Figure 2. Schematic representation of the hydrogen-bond energy its components and wave functions used to calculate them.

$$\phi_{14} = \{0.0807(\text{H}_1^{\text{F}} + \text{H}_2^{\text{F}}) - 0.0032(\text{O}_{1s}^{\text{F}}) + 0.0144(\text{O}_{2s}^{\text{F}}) - 0.0865(\text{O}_x^{\text{F}}) + 0.7596(\text{O}_z^{\text{F}}) + 0.0401(\text{C}_{1s}^{\text{F}}) - 0.2063(\text{C}_{2s}^{\text{F}}) + 0.0908(\text{C}_z^{\text{F}}) - 0.7220(\text{C}_z^{\text{F}})\} + \{-0.0437(\text{H}_1^{\text{W}}) - 0.0224(\text{H}_2^{\text{W}}) - 0.0089(\text{O}_{1s}^{\text{W}}) + 0.0535(\text{O}_{2s}^{\text{W}}) + 0.0610(\text{O}_x^{\text{W}}) - 0.1542(\text{O}_z^{\text{W}})\}$$

Or expanding them in terms of the occupied and vacant MO's of the ground state SCF calculation

$$\phi_{13} = 0.2083\psi_7 + 0.4568\psi_{12} - 0.8649\psi_{13}$$

$$\phi_{14} = 0.9948\psi_{14} + 0.0678\psi_{15} - 0.0369\psi_{16} + 0.0226\psi_{18} - 0.0631\psi_{19}$$

One can clearly see that ϕ_{13} is almost completely localized on H₂CO and looks like the highest occupied n MO of the isolated H₂CO and that ϕ_{14} is also strongly localized on H₂CO and is essentially the lowest vacant "π*" type MO of the isolated H₂CO. Of course, the EHP picture is more realistic than the virtual MO picture when one is discussing such a weak interaction as the hydrogen bonding.

C. Decomposition of the Hydrogen-Bond Energy.

In order to understand the mechanism and the character of the hydrogen bonding, it is very useful to decompose the stabilization energy gained by the bond formation into the electrostatic (E_{es}), electron-exchange repulsion (E_{ex}), polarization (E_{p1}), resonance (E_{rs}), and charge-transfer (E_{ct}) energies. The scheme proposed by one of the authors for the ground state has to be extended in order to apply for the excited states. Figure 2 illustrates the proposed scheme.

At the infinite separation, the isolated molecules, a formaldehyde F and a water W, have wave functions $\Phi_0^{\text{F}_i}$ and $\Phi_0^{\text{W}_0}$, respectively, where the superscript F_i denotes the i th state of formaldehyde and W_0 the ground state of water. Each wave function is antisymmetrized. The sum of total energies of the isolated molecules is E_0^i .

When the molecules approach each other, the following wave functions can be defined and energies associated with them can be calculated.

(i) **The Hartree Product $\Phi_0^{\text{F}_i} \Phi_0^{\text{W}_0}$ of the Molecular Wave Function Determined at Infinite Separation.** The energy associated with this product is called E_1^i .

The difference between E_1^i and E_0^i is the pure electrostatic interaction energy between two molecules.

$$E_{es} = -(E_1^i - E_0^i) \quad (9)$$

The interaction is defined as positive when the stabilization is resulted.

(ii) **The Hartree Product $\Phi^F_i\Phi^W_0$ of Two Molecular Wave Functions Which Are Optimized by the EHP Procedure in the Electrostatic Field of the Other Molecule.** The energy is E_2^i . This is most conveniently accomplished in the AO integral evaluation by neglecting all the differential overlaps between AO's belonging to different molecules and then carrying out the regular HF and EHP procedures on the entire system.

In order to facilitate the understanding of contributions included in E_2^i , it is convenient to expand the wave functions $\Phi^F_i\Phi^W_0$ in terms of products of wave functions of isolated molecules

$$\begin{aligned} \Phi^F_i\Phi^W_0 &= \Phi_0^F_i\Phi_0^W_0 + \\ &\sum_{j \neq i} \frac{\langle F_j W_0 | V | F_i W_0 \rangle}{E(F_i W_0) - E(F_j W_0)} \Phi_0^F_j \Phi_0^W_0 + \dots + \\ &\sum_{k \neq 0} \frac{\langle F_i W_k | V | F_i W_0 \rangle}{E(F_i W_0) - E(F_i W_k)} \Phi_0^F_i \Phi_0^W_k + \\ &\sum_{j \neq i} \sum_{k \neq 0} \frac{\langle F_j W_k | V | F_i W_0 \rangle}{E(F_i W_0) - E(F_j W_k)} \Phi_0^F_j \Phi_0^W_k + \dots \quad (10) \end{aligned}$$

where V is the interaction potential in the Hamiltonian, $E(F_i W_0)$ is the energy associated with the wave function $\Phi_0^F_i\Phi_0^W_0$ at this geometry, and $\langle F_j W_0 | V | F_i W_0 \rangle$ is the matrix element of V between $\Phi_0^F_j\Phi_0^W_0$ and $\Phi_0^F_i\Phi_0^W_0$. Then the interaction energy associated with $\Phi^F_i\Phi^W_0$, eq 10, can be written as

$$\begin{aligned} \langle \Phi^F_i\Phi^W_0 | V | \Phi^F_i\Phi^W_0 \rangle &= \langle F_i W_0 | V | F_i W_0 \rangle + \\ &2 \sum_{j \neq i} \frac{|\langle F_j W_0 | V | F_i W_0 \rangle|^2}{E(F_i W_0) - E(F_j W_0)} + 2 \sum_{k \neq 0} \frac{|\langle F_i W_k | V | F_i W_0 \rangle|^2}{E(F_i W_0) - E(F_i W_k)} + \\ &2 \sum_{j \neq i} \sum_{k \neq 0} \frac{|\langle F_j W_k | V | F_i W_0 \rangle|^2}{E(F_i W_0) - E(F_j W_k)} + \dots \quad (11) \end{aligned}$$

The first term on the right-hand side is the electrostatic interaction E_{es} . The second and third terms involve the induction energy, the interaction between the permanent dipole and the dipole induced by it. The fourth term involves the transition between the original state $\Phi_0^F_i\Phi_0^W_0$ to a state $\Phi_0^F_j\Phi_0^W_k$, in which both molecules changed the quantum numbers, and is the interaction between induced dipole moments. The last three terms constitute the polarization energy.¹⁷

For the interaction between a ground state molecule and an excited state molecule, particular terms ($j = 0$, ground state) of the fourth term of eq 11 become ex-

$$2 \sum_k \frac{|\langle F_0 W_k | V | F_i W_0 \rangle|^2}{E(F_i W_0) - E(F_0 W_k)} \quad (12)$$

remely important. These involve an excitation energy transfer from formaldehyde (F), which is deexcited from i to 0, to water (W), which is excited from 0 to k . If interacting molecules are identical, as in the case of a dimer, the denominator becomes zero when $k = i$, and the interaction energy becomes of the first order. This

(17) It is believed that dispersion force is not included in the Hartree-Fock approximation. See Appendix A in ref 18d.

situation is called (intermolecular) resonance.¹⁸ Even if interacting molecules are different as in this formaldehyde-water case, the term of eq 12, which we may call the resonance energy,¹⁸ may make an important contribution. Two characteristic features should be noted for the resonance energy. At first the numerator has a nonzero Coulomb term only when F_i and W_k are both singlet states, because F_0 and W_0 are both the ground states of closed shell molecules. So there is little resonance stabilization for the triplet state formaldehyde upon hydrogen bonding. Second, a large contribution comes from the term which satisfies

$$E(F_i W_0) - E(F_0 W_k) \sim 0$$

Therefore, the contribution is very dependent on the excited state i of formaldehyde.

The polarization energy (for excited states, combined with resonance energy) is called E_{pr}^i . E_2^i includes E_{es}^i as well as E_{pr}^i .

$$-(E_2 - E_0) = E_{es}^i + E_{pr}^i$$

By using eq 9, one obtains E_{pr}^i .

$$E_{pr}^i = -(E_1^i - E_1^0) \quad (13)$$

(iii) **The Antisymmetrized Product α ($\Phi_0^F_i\Phi_0^W_0$) of Two Molecular Wave Functions Determined at Infinite Separation.** The energy is E_3^i . The antisymmetrizer α exchanges electrons of formaldehyde with those of water. E_3^i should include the electrostatic energy E_{es}^i plus the exchange repulsion energy E_{ex}^i (a negative quantity) between two electron clouds. Thus

$$-(E_3^i - E_0^i) = E_{es}^i + E_{ex}^i$$

From eq 9

$$E_{ex}^i = -(E_3^i - E_1^i) \quad (14)$$

MO's in $\Phi_0^F_i$ are not in general orthogonal to MO's in Φ_0^W . For the ground state of the combined system E_3 is calculated by orthogonalizing occupied MO's between W and F and then calculating the expectation value of the Hamiltonian. For excited states the method described in the Appendix is used.

(iv) **The EHP Wave Function for the Whole System Φ_{FW}^i** (if i is the ground state, of course the SCF wave function Φ_{FW}^0). The energy is E_4^i . The total hydrogen-bonding energy E_H^i is of course defined as

$$E_H^i = -(E_4^i - E_0^i) \quad (15)$$

The energy E_H^i can be looked upon as the sum of all the contributions including the change-transfer or electron-delocalization energy E_{ct} between two molecules.

$$E_H^i = -(E_4^i - E_0^i) = E_{es}^i + E_{pr}^i + E_{ex}^i + E_{ct}^i$$

From eq 15

$$E_{ct}^i = E_H^i - (E_{es}^i + E_{pr}^i + E_{ex}^i) \quad (16)$$

If E_2^i is not calculated, instead of separate E_{pr}^i and E_{ct}^i , one obtains their sum

$$E_{pr}^i + E_{ct}^i = E_H^i - (E_{es}^i + E_{ex}^i) \quad (17)$$

(18) (a) H. Margenau, *Rev. Mod. Phys.*, **11**, 1 (1939); (b) J. O. Hirschfelder, C. F. Curtis, and R. B. Bird, "Theory of Gases and Liquids," Wiley, New York, N. Y., 1964; (c) J. O. Hirschfelder, Ed., "Advances in Chemical Physics," Vol. 12, Interscience, New York, N. Y., 1967; (d) H. Margenau and N. R. Kestner, "Theory of Intermolecular Forces," 2nd ed, Pergamon Press, New York, N. Y., 1971.

Table I. Vertical Excitation Energies and Total Energies of Formaldehyde

State	Vertical excitation energy, eV			Exptl	Total energy, hartrees	
	Present EHP				Minimum STO	
	Mini- mum STO	STO-3G ^a + diffuse p	Large basis ^b SCF-CI		Planar	Bent
Ground					-113.47822	-113.44486
³ n-π*	3.11	3.61	3.41	3.12 ^c	-113.36415	-113.38358
¹ n-π*	4.21	4.42	3.81	3.50 ^c	-113.32355	-113.33875
³ π-π*	4.06	4.88	5.56		-113.32929	-113.39296
¹ σ-π*	9.35	9.36	9.03	~9.0 ^d	-113.13487	-113.18154
¹ π-π*	15.12	12.08	11.41		-112.92278	

^a The exponents of the diffuse Gaussian are 0.06 and 0.106 for carbon and oxygen, respectively.²⁴ ^b Reference 19. ^c Reference 12. ^d Reference 20.

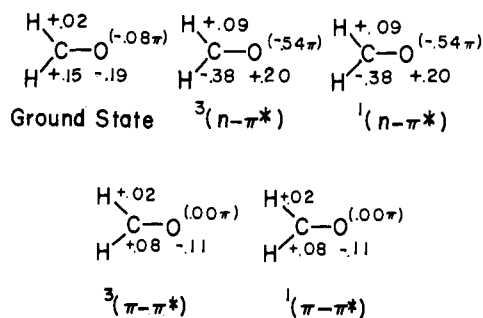


Figure 3. Electron populations on atoms for various states of formaldehyde in the planar ground state geometry.

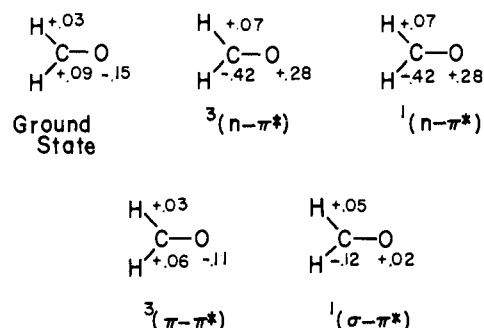


Figure 4. Electron population on the atom for various states of formaldehyde in the bent geometry.

It should be mentioned that in the EHP method the above energy decomposition, especially the calculation of E_3^i , is much easier than in the CI method, since the EHP wave function is a single configuration function.

As will be seen in section III, the energy components of the hydrogen-bond energy are more sensitive than the hydrogen-bond energy itself to the choice of basis sets. Despite this, one sees that the comparison of the decomposition between different states or different geometries within a given basis set is still revealing in studying the origins of hydrogen bonding.

II. Results

A. The Excited States of Formaldehyde by the EHP Method. A number of articles have recently appeared in which *ab initio* SCF-MO-CI calculations were performed for some of the lower excited states of the formaldehyde molecule.^{13-15,19,20} We first compare the EHP results with the CI results for an isolated formaldehyde molecule in Table I.

The electronic configurations of the ground state for the planar (C_{2v}) and bent (C_s) formaldehyde are, respectively

$$\dots(3a_1)^2(4a_1)^2(1b_2)^2(5a_1)^2(1b_1)^2(2b_2)^2$$

$$\dots(3a')^2(4a')^2(1a'')^2(5a')^2(6a')^2(2a'')^2$$

where the molecular orbitals are arranged in the order of increasing orbital energy. The MO $2b_2(2a'')$ is essentially the lone pair orbital (called n) of the oxygen atom, the MO $1b_1(6a')$ is the π orbital, and the MO $5a_1(5a')$ is essentially the C=O bonding σ orbital (called σ). The lowest vacant MO $2b_1(7a')$ is essentially the

π^* antibonding orbital (called π^* for convenience both in planar and nonplanar structures). In the planar molecule the n- π^* ($2b_2 \rightarrow 2b_1$), π - π^* ($1b_1 \rightarrow 2b_1$), and σ - π^* ($5a_1 \rightarrow 2b_1$) states have A_2 , A_1 , and B_1 symmetries, respectively, while in the bent form the π - π^* and σ - π^* states belong to the same irreducible representation A' . Since the EHP method is based on the variation principle, the method is rigorously applicable only for the lowest excited state of a given symmetry but not for higher states. Therefore, for the bent formaldehyde models calculations are limited to the n- π^* singlet and triplet states, the σ - π^* ($5a' \rightarrow 7a'$) singlet, and the π - π^* ($6a' \rightarrow 7a'$) triplet states, the latter two being the lowest singlet and triplet states of the A' symmetry, respectively.

In comparing the sixth column of Table I with the seventh, the bent structure is found to be more stable in all excited states treated. A fault of the EHP method with the minimal basis set, which also appears in the one-electron excited configuration interaction calculation,¹⁵ is that the π - π^* triplet state is lower than the n- π^* triplet state in the planar and bent structures. In order to avoid this fault, the diffuse orbitals have to be added, or doubly excited configurations have to be taken into account.^{13,14}

It is now well established that the minimum STO basis set is unable to describe the singlet π - π^* and σ - π^* excited states appropriately.^{13,14,19,20} Diffuse p orbitals are required to make the calculated energy agree with experiments, and the resultant π - π^* singlet state is a diffuse Rydberg-like state. Therefore, the hydrogen-bond energy calculation for the $^1(\sigma$ - $\pi^*)$ and $^1(\pi$ - $\pi^*)$ states in section II should be considered as a model calculation. In section III we will discuss the effect of basis functions more explicitly.

(19) D. S. Peyerimhoff, R. J. Buenker, W. E. Kammer, and H. Hsu, *Chem. Phys. Lett.*, **8**, 129 (1971).

(20) J. E. Mentall, E. P. Gientew, M. Krauss, and D. Neumann, *J. Chem. Phys.*, **55**, 5471 (1971).

Table II. Hydrogen-Bond Energy, Its Components (in kcal/mol) and the Charge Transfer ΔQ in PH and BH Models at $\theta = 60^\circ$

Model no. (geometry)	State	E_H	E_{es}	E_{ex}	E_{pr}	E_{ct}	$E_{pr} + E_{ct}$	ΔQ
PH 1 ($\theta = 60^\circ$, $R_{OH} = 1.797 \text{ \AA}$)	Ground	3.3	5.8	-19.8	0.2	17.1	17.3	0.0302
	$^3(n-\pi^*)$	-1.9	0.4	-18.2	1.6	14.4	6.0	0.0174
	$^1(n-\pi^*)$	-0.6	0.5	-18.1	2.2	14.9	17.1	0.0163
	$^3(\pi-\pi^*)$	1.8	5.0	-19.9	0.1	16.7	16.7	0.0302
	$^1(\sigma-\pi^*)$	0.6	1.1	-18.6	1.4	16.9	18.3	0.0108
PH 2 ($\theta = 60^\circ$, $R_{OH} = 1.946 \text{ \AA}$)	Ground	3.4	4.1	-10.8	0.2	9.9	10.1	0.0197
	$^3(n-\pi^*)$	-0.7	-0.2	-9.9	1.3	8.1	9.4	0.0113
	$^1(n-\pi^*)$	0.2	-0.1	-9.9	1.6	8.6	10.2	0.0108
	$^3(\pi-\pi^*)$	2.2	3.4	-10.9	0.1	9.7	9.7	0.0196
	$^1(\sigma-\pi^*)$	0.8	0.3	-10.1	1.1	9.6	10.7	0.0093
BH 1 ($\theta = 60^\circ$, $R_{OH} = 1.946 \text{ \AA}$)	Ground	3.5	4.0	-10.7	0.2	10.0	10.3	0.0209
	$^3(n-\pi^*)$	-1.3	-1.1	-9.8	1.7	8.0	9.7	0.0114
	$^1(n-\pi^*)$	-0.0	-1.1	-9.8	2.1	8.7	10.8	0.0107
	$^3(\pi-\pi^*)$	2.6	3.6	-10.8	0.0	9.8	9.8	0.0209
	$^1(\sigma-\pi^*)$	1.2	-0.7	-9.1	2.5	8.5	11.0	0.0135
BH 2 ($\theta = 60^\circ$, $R_{OH} = 2.30 \text{ \AA}$)	Ground	2.4	2.1	-2.5	0.1	2.6	2.8	0.0060
	$^3(n-\pi^*)$	-0.3	-1.1	-2.3	1.1	2.0	3.1	0.0035
	$^1(n-\pi^*)$	0.2	-1.1	-2.3	1.4	2.1	3.6	0.0033
	$^3(\pi-\pi^*)$	1.9	1.8	-2.5	0.0	2.6	2.6	0.0060
	$^1(\sigma-\pi^*)$	0.8	-0.1	-2.4	0.8	2.4	3.2	0.0043

Table III. Hydrogen-Bond Energy, Its Components (in kcal/mol) and the Charge Transfer ΔQ in PH and BH Models

Model no. (geometry)	State	E_H	E_{es}	E_{ex}	$E_{pr} + E_{ct}$	ΔQ
PH 3 ($\theta = 30^\circ$, $R_{OH} = 1.797 \text{ \AA}$)	Ground	2.4	5.7	-18.4	15.2	0.0275
	$^3(n-\pi^*)$	-1.1	1.6	-18.3	15.6	0.0220
	$^1(n-\pi^*)$	-0.2	1.7	-18.2	16.3	0.0222
	$^3(\pi-\pi^*)$	1.4	5.1	-18.6	14.8	0.0275
	$^1(\pi-\pi^*)$	2.9	5.1	-18.5	16.4	0.0275
PH 4 ($\theta = 30^\circ$, $R_{OH} = 2.096 \text{ \AA}$)	Ground	2.5	2.8	-5.4	5.1	0.0103
	$^3(n-\pi^*)$	0.3	0.0	-5.3	5.6	0.0086
	$^1(n-\pi^*)$	0.8	0.1	-5.3	6.0	
	$^3(\pi-\pi^*)$	1.8	2.3	-5.4	4.9	0.0103
	$^1(\pi-\pi^*)$	2.7	2.3	-5.4	5.7	0.0102
PH 5 ($\theta = 30^\circ$, $R_{OH} = 2.5 \text{ \AA}$)	Ground	1.7	1.6	-1.0	1.1	0.0023
	$^3(n-\pi^*)$	0.5	-0.3	-1.0	1.7	0.0019
	$^1(n-\pi^*)$	0.8	-0.2	-1.0	1.9	0.0019
	$^3(\pi-\pi^*)$	1.3	1.2	-1.0	1.0	0.0023
	$^1(\pi-\pi^*)$	1.8	1.2	-1.0	1.5	0.0023
PH 6 ($\theta = 45^\circ$, $R_{OH} = 1.797 \text{ \AA}$)	Ground	2.9	5.7	-9.0	16.2	0.0302
	$^3(n-\pi^*)$	-1.4	1.0	-18.0	15.7	0.0204
	$^1(n-\pi^*)$	-0.3	1.1	-17.9	16.5	0.0196
	$^3(\pi-\pi^*)$	1.7	5.1	-19.1	15.7	0.0302
	$^1(\pi-\pi^*)$	3.3	5.1	-19.1	17.4	0.0300
PH 7 ($\theta = 75^\circ$, $R_{OH} = 1.797 \text{ \AA}$)	Ground	3.0	5.8	-21.9	19.1	0.0310
	$^3(n-\pi^*)$	-2.9	-0.0	-20.2	17.3	0.0141
	$^1(n-\pi^*)$	-1.6	0.1	-20.2	18.5	0.0129
	$^3(\pi-\pi^*)$	1.2	4.9	-22.1	18.4	
	$^1(\pi-\pi^*)$	3.0	4.9	-22.1	20.2	0.0307
BH 3 ($\theta = 0^\circ$, $R_{OH} = 2.3 \text{ \AA}$)	Ground	1.7	1.7	-2.7	2.7	0.0043
	$^3(n-\pi^*)$	0.2	-0.7	-2.3	3.2	0.0043
	$^1(n-\pi^*)$	0.5	-0.7	-2.3	3.5	0.0043
	$^3(\pi-\pi^*)$	1.4	1.5	-2.2	2.1	0.0043
	$^1(\sigma-\pi^*)$	-0.2	-0.9	-1.7	2.4	0.0030
BH 4 ($\theta = 30^\circ$, $R_{OH} = 2.3 \text{ \AA}$)	Ground	1.9	1.8	-2.3	2.4	0.0050
	$^3(n-\pi^*)$	0.0	-1.0	-2.3	3.2	0.0041
	$^1(n-\pi^*)$	0.5	-0.9	-2.3	3.7	0.0041
	$^3(\pi-\pi^*)$	1.6	1.6	-2.3	2.3	0.0050
	$^1(\sigma-\pi^*)$	-0.1	-0.9	-1.4	2.1	0.0017

Electron populations for each state of planar and bent formaldehyde are shown in Figures 3 and 4, respectively. The H₂O molecule with the present basis set has the following atomic populations: H (+0.21) and O (-0.42).

B. Hydrogen Bond with H₂O in the Molecular Plane of H₂CO (PH and BH Models). Calculated results for

PH and BH models where the water molecule lies in the H₂CO molecular (xy) plane are shown in Tables II and III. Figures 5 and 6 show E_{es} , E_{ex} , $E_{pr} + E_{ct}$, and E_H as functions of the hydrogen-bond length R_{OH} at $\theta = 30^\circ$ and of θ at $R_{OH} = 1.797 \text{ \AA}$, respectively, for PH models. As can be seen in Table II, almost no hydrogen-bond energy is gained for the $n-\pi^*$ singlet

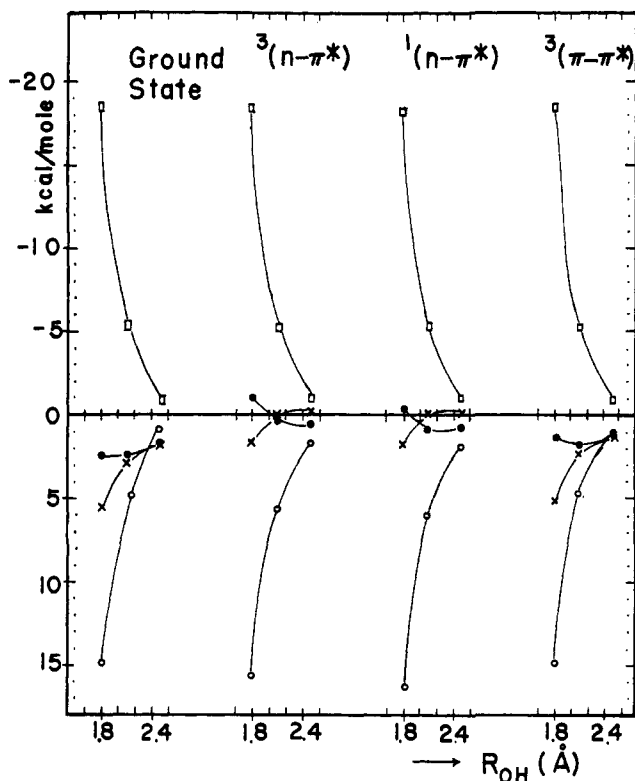


Figure 5. Hydrogen-bond energy and its components as functions of the hydrogen-bond distance R_{OH} for PH models at $\theta = 30^\circ$: (—●—) E_H (total hydrogen-bond energy); (—×—) E_{es} (electrostatic energy); (—□—) E_{ex} (exchange repulsion); (—○—) $E_{pr} + E_{ct}$ (polarization and charge-transfer energy).

and triplet and $\sigma-\pi^*$ singlet states in the neighborhood of the most stable geometry of the ground state: PH ($\theta = 64^\circ$, $R_{OH} = 1.89 \text{ \AA}$). This is consistent with the well-known observed blue shift of $n-\pi^*$ transitions.

The origin of the blue shift can be understood by the full energy decomposition for PH 1 and PH 2 models (Table II) and by Figure 4. The major factor is obviously the only slight attractive or repulsive electrostatic energy E_{es} in the $n-\pi^*$ states, in which the oxygen atom of formaldehyde is positively charged (Figure 2). Another factor is the decrease upon excitation of the charge-transfer stabilization energy E_{ct} which exceeds the decrease of the exchange repulsion energy E_{ex} (Table II). The depletion of the donor electron upon the $n-\pi^*$ excitation causes this decrease of charge-transfer and exchange-repulsion energies. This is also reflected by the fact in Table II that the amount of charge transfer ΔQ from formaldehyde to water in the $n-\pi^*$ states is about half of that in the ground state.

Another interesting feature is the rather large polarization energy in the $n-\pi^*$ states. Since E_{pr} contains no resonance effect for the triplet state as discussed in section IC, $E_{pr} = 1.6 \text{ kcal/mol}$ for the ${}^3(n-\pi^*)$ state of the PH1 model compared with 0.2 kcal/mol for the ground state and 0.1 kcal for the ${}^3(\pi-\pi^*)$ state gives an example. This is probably due to the presence of a strongly allowed, low-energy transition from the $n-\pi^*$ state to the $n\pi-\pi^*\pi^*$ state. The difference of E_{pr} between the singlet and triplet state should give a rough estimate of the resonance energy, if MO's in both states are the same (and this is qualitatively true for $n-\pi^*$ states of formaldehyde). For the $n-\pi^*$ singlet state

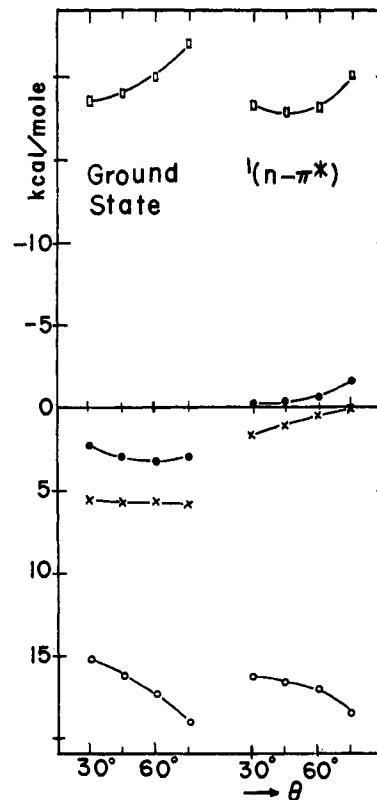


Figure 6. Hydrogen-bond energy and its components as functions of the angle θ for PH models at $R_{OH} = 1.797 \text{ \AA}$. For notations, see Figure 5. ${}^3(n-\pi^*)$ is almost the same as ${}^1(n-\pi^*)$.

of the PH 1 model the resonance energy thus estimated from Table II is 0.6 kcal/mol .

The potential curve of the $n-\pi^*$ states as functions of the angle θ shows a minimum around 30° , which is smaller than 64° in the ground state (Figure 5 and Tables II and III). The most important factor is again the electrostatic energy.

As mentioned in section IIA, minimal basis calculations cannot accurately describe the $\sigma-\pi^*$ singlet state, which involves a more diffuse π^* orbital. Therefore, we do not take results in Tables II and III for this state seriously as corresponding to any real low-lying state. But it is interesting to notice that the energy decomposition for this state is very similar to that of the ${}^1(n-\pi^*)$ state.

The hydrogen-bond energy, its geometry dependence, and decomposition characteristics for the $\pi-\pi^*$ states are very similar to those of the ground state. This is not surprising because the σ and n electron distribution of the former is not much different from that of the latter, and the hydrogen bonding in this model takes place within the plane of H_2CO . We note again that the actual low-lying $\pi-\pi^*$ singlet state involves diffuse p orbitals and the present STO calculating does not correspond to such diffuse states (see Table XI for such calculations).

A small change of the hydrogen-bond energy and a small blue shift of the vertical transition energy in the $\pi-\pi^*$ triplet state comes from the decrease of the electrostatic and charge-transfer energies. If one assumes that MO's of the $\pi-\pi^*$ singlet state are very close to those of the $\pi-\pi^*$ triplet state, the resonance energy for the $\pi-\pi^*$ singlet state is estimated to be about 1.0 kcal/mol for the PH 1 model.

Table IV. Hydrogen-Bond Energy, Its Components (kcal/mol) and the Charge Transfer in PV-O Models

Model no. (geometry)	State	E_H	E_{es}	E_{ex}	$E_{pr} + E_{ct}$ (E_{pr}, E_{ct})	ΔQ
PV-O 1 ($R_{BH} = 1.797 \text{ \AA}$, $\gamma = 90^\circ$, $\phi = 0^\circ$)	Ground	-2.5	3.2	-12.6	6.9	0.0310
	$^3(n-\pi^*)$	-4.1	1.9	-13.2	7.2	0.0317
	$^1(n-\pi^*)$	-3.1	2.0	-12.2	7.2	0.0321
	$^3(\pi-\pi^*)$	-3.8	1.0	-6.9	2.1	0.0071
	$^1(\sigma-\pi^*)$	-3.3	1.9	-12.9	7.8	0.0289
PV-O 2 ($R_{BH} = 2.096 \text{ \AA}$, $\gamma = 90^\circ$, $\phi = 0^\circ$)	Ground	-0.1	1.2	-8.7	7.4	0.0131
	$^3(n-\pi^*)$	-0.8	0.2	-8.9	7.8	0.0132
	$^1(n-\pi^*)$	-0.3	0.3	-8.9	8.3	0.0132
	$^3(\pi-\pi^*)$	-1.5	-0.0	-6.6	5.2	0.0038
	$^1(\sigma-\pi^*)$	-0.6	0.2	-8.8	8.0	0.0125
PV-O 3 ($R_{BH} = 2.30 \text{ \AA}$, $\gamma = 90^\circ$, $\phi = 0^\circ$)	Ground	0.3	0.7	-4.0	3.6	0.0069
	$^3(n-\pi^*)$	-0.1	-0.1	-4.1	(0.1, 3.5) 4.0	0.0069
	$^1(n-\pi^*)$	0.3	0.0	-4.1	(0.7, 3.4) 4.3	0.0069
	$^3(\pi-\pi^*)$	-0.7	-0.1	-3.0	(0.9, 3.4) 2.4	0.0022
	$^1(\sigma-\pi^*)$	-0.0	-0.1	-3.9	(0.0, 2.3) 4.0 (0.7, 3.2)	0.0066

Table V. Hydrogen-Bond Energy, Its Components (kcal/mol) and the Charge Transfer in BV-O Models with $\gamma = 90^\circ$

Model no. (geometry)	State	E_H	E_{es}	E_{ex}	$E_{pr} + E_{ct}$	ΔQ
BV-O 1 ($R_{BH} = 1.89 \text{ \AA}$, $\gamma = 90^\circ$, $\phi = 0^\circ$)	Ground	-0.0	2.4	-17.5	15.1	0.0277
	$^3(n-\pi^*)$	-2.6	0.3	-18.2	15.3	0.0283
	$^1(n-\pi^*)$	-1.6	0.3	-19.2	17.4	0.0285
	$^3(\pi-\pi^*)$	-2.5	1.0	-13.7	10.2	0.0098
	$^1(\sigma-\pi^*)$	-0.8	1.1	-16.5	14.6	0.0247
BV-O 2 ($R_{BH} = 2.30 \text{ \AA}$, $\gamma = 90^\circ$, $\phi = 0^\circ$)	Ground	0.9	0.9	-2.8	2.8	0.0081
	$^3(n-\pi^*)$	-0.1	-0.4	-3.8	4.2	0.0082
	$^1(n-\pi^*)$	0.4	-0.4	-3.8	4.6	
	$^3(\pi-\pi^*)$	-0.4	0.3	-2.7	2.0	0.0031
	$^1(\sigma-\pi^*)$	0.1	0.1	-3.7	3.0	0.0075
BV-O 3 ($R_{BH} = 2.50 \text{ \AA}$, $\gamma = 90^\circ$, $\phi = 0^\circ$)	Ground	0.8	0.7	-1.0	1.2	0.0041
	$^3(n-\pi^*)$	0.1	-0.5	-2.2	2.8	0.0042
	$^1(n-\pi^*)$	0.4	-0.5	-2.2	3.1	0.0042
	$^3(\pi-\pi^*)$	-0.2	0.1	-1.1	0.8	0.0016
	$^1(\sigma-\pi^*)$	0.5	-0.0	-1.7	2.3	0.0039

Roughly speaking, the difference in the exchange repulsion energy between various states for a given geometry is rather small. This is probably because the exchange repulsion is caused by the overlap of two electron clouds in a close approach and does not depend sensitively on the detail of the clouds. Going into details, one finds that the exchange repulsion in the $n-\pi^*$ and $\sigma-\pi^*$ states is a little smaller than in other states, which may be due to the absence of the n or σ electron cloud in the former states.

The hydrogen-bond energy in the bent $n-\pi^*$ state is smaller than in the planar $n-\pi^*$ state, as seen in models BH 1 and PH 2 in Table II. A smaller electrostatic energy is responsible for this result.

C. π -Hydrogen Bonding Over the Oxygen Atom (PV-O and BV-O Models). Tables IV and V show the results for the π -hydrogen bond to the oxygen atom of the planar (PV-O models) and bent (BV-O models) formaldehyde, respectively. All states in these models are unstable at such a short bond distance where the ground state has a minimum. The energy decomposition makes it clear that a large exchange repulsion E_{ex} and a small electrostatic stabilization E_{es} lead to the instability of the π -hydrogen bonding over an oxygen atom.

At a larger distance, around 2.3 \AA , the ground, $^1(n-\pi^*)$, $^3(n-\pi^*)$, and $^1(\sigma-\pi^*)$ (the last two in the BV model only) states show a small positive hydrogen-bond energy. The $\pi-\pi^*$ triplet state is always repulsive in all the PV-O and BV-O models, because here E_{ex} , $E_{pr} + E_{ct}$, and ΔQ are much smaller than in other states. One also notes that the component E_{es} changes from positive (attractive) to negative (repulsive) with the increasing bond distance R_{OH} in most excited states.

In order to search the stable position for the oxygen coordination for the $n-\pi^*$ state, the angle γ was changed with a fixed distance $R_{BH} = 2.3 \text{ \AA}$ for the bent (BV-O) model. As shown in Table VI, there is no or little stabilization for the $n-\pi^*$ and $\sigma-\pi^*$ states because of the repulsive electrostatic energy E_{es} , even though the stabilization $E_{ct} + E_{pr}$ exceeds the other repulsion E_{ex} .

D. π -Hydrogen Bonding Over the C-O Bond (PV-M and BV-M Models) and Over the Carbon Atom (PV-C and BV-C Models). In the ground state the π -hydrogen bonding with H_2O approaching the C-O bond has been found to be almost nonbonding.¹ As can be seen in Table VII, all the excited states of the planar H_2CO models (PV-M Models) show little or no hydrogen-bond energy. The bent (BV-M) models are more bonding, except for the $\pi-\pi^*$ triplet state.

Table VI. Hydrogen-Bond Energy, Its Components (kcal/mol) and the Charge Transfer for BV-O Models with $\gamma \neq 90^\circ$

Model no. (geometry)	State	E_H	E_{es}	E_{ex}	$E_{pr} + E_{ct}$	ΔQ
BV-O 5 ($R_{BH} = 2.30 \text{ \AA}$, $\gamma = 60^\circ$, $\phi = 0^\circ$)	Ground	1.6	1.4	-2.2	2.4	0.0046
	$^3(n-\pi^*)$	0.1	-0.8	-2.4	3.3	0.0052
	$^1(n-\pi^*)$	0.6	-0.8	-2.4	3.8	0.0054
	$^3(\pi-\pi^*)$	0.7	0.9	-2.0	1.8	0.0035
	$^1(\sigma-\pi^*)$	0.3	0.7	-2.1	3.1	0.0031
BV-O 6 ($R_{BH} = 2.30 \text{ \AA}$, $\gamma = 30^\circ$, $\phi = 0^\circ$)	Ground	1.8	1.7	-2.2	2.3	0.0044
	$^3(n-\pi^*)$	0.2	-0.8	-2.3	3.3	0.0046
	$^1(n-\pi^*)$	0.6	-0.8	-2.3	3.6	0.0047
	$^3(\pi-\pi^*)$	1.3	1.4	-2.1	2.0	0.0041
	$^1(\sigma-\pi^*)$	-0.2	-1.1	-1.8	2.7	0.0008
BV-O 7 ($R_{BH} = 2.30 \text{ \AA}$, $\gamma = 60^\circ$, $\phi = 0^\circ$)	Ground	1.3	1.1	-2.1	2.3	0.0041
	$^3(n-\pi^*)$	-0.1	1.0	-2.4	3.3	0.0049
	$^1(n-\pi^*)$	0.4	-1.0	-2.4	3.7	0.0051
	$^3(\pi-\pi^*)$	0.7	0.8	-2.0	1.9	0.0035
	$^1(\sigma-\pi^*)$	0.5	-0.4	-2.3	3.1	0.0045
BV-O 8 ($R_{BH} = 2.30 \text{ \AA}$, $\gamma = -90^\circ$, $\phi = 0^\circ$)	Ground	0.5	0.6	-3.8	3.7	0.0073
	$^3(n-\pi^*)$	-0.6	-1.0	4.0	4.3	0.0073
	$^1(n-\pi^*)$	-0.2	-0.9	-4.0	4.8	0.0074
	$^3(\pi-\pi^*)$	-0.6	-0.0	-3.0	2.5	0.0030
	$^1(\sigma-\pi^*)$	0.1	-0.2	-3.9	4.3	0.0074

Table VII. Hydrogen-Bond Energy, Its Components (kcal/mol) and the Charge Transfer for PV-M and BV-M Models

Model no. (geometry)	State	E_H	E_{es}	E_{ex}	$E_{pr} + E_{ct}$	ΔQ
PV-M 1 ($R_{BH} = 2.30 \text{ \AA}$)	Ground	-0.8	0.2	-5.6	4.7	0.0081
	$^3(n-\pi^*)$	-0.1	0.6	-5.9	5.2	0.0105
	$^1(n-\pi^*)$	0.0	0.7	-5.9	5.2	0.0103
	$^3(\pi-\pi^*)$	-1.6	-0.6	-4.4	3.4	0.0030
	$^1(\sigma-\pi^*)$	-0.2	0.5	-5.9	5.1	0.0098
PV-M 2 ($R_{BH} = 2.80 \text{ \AA}$)	Ground	-0.0	0.0	-0.8	0.8	0.0015
	$^3(n-\pi^*)$	0.2	0.1	-0.9	1.0	0.0020
	$^1(n-\pi^*)$	0.3	0.1	-0.9	1.1	0.0020
	$^3(\pi-\pi^*)$	-0.6	-0.5	-0.7	0.6	0.0008
	$^1(\sigma-\pi^*)$	0.1	0.0	-0.9	1.0	0.0019
BV-M 1 ($R_{BH} = 2.50 \text{ \AA}$)	Ground	0.2	0.3	-2.5	2.4	0.0056
	$^3(n-\pi^*)$	0.6	0.4	-2.6	2.8	0.0071
	$^1(n-\pi^*)$	0.6	0.4	-2.6	2.8	0.0069
	$^3(\pi-\pi^*)$	-0.8	-0.3	-1.8	1.3	0.0025
	$^1(\sigma-\pi^*)$	0.8	0.7	-2.6	2.7	0.0065

The analysis indicates that in these models E_{es} is very small and the balance of large E_{ex} and $E_{pr} + E_{ct}$ determines whether the net result is bonding or not. Table VII also suggests that the more antibonding behavior of the $\pi-\pi^*$ triplet state is due to the repulsive E_{es} and the smaller $E_{pr} + E_{ct}$ compared with E_{ex} .

When the hydrogen atom of H_2O approaches the carbon atom of H_2CO , the $n-\pi^*$ singlet and triplet and $\sigma-\pi^*$ singlet states gain the hydrogen-bond energy. As is seen in Tables VIII and IX, this is more enhanced for the bent H_2CO (BV-C models) than for the planar H_2CO (PV-C models). The most stable geometry for these states was found around at the bond distance $R_{BH} \sim 2.3 \text{ \AA}$ and the angle $\alpha \sim 15^\circ$ (Table IX). In fact, for these states this is the most stable of the models we have studied. The present results suggest that the $n-\pi^*$ excited states in their bent equilibrium geometry would have a weak hydrogen bonding on the carbon atom to form a tetrahedral structure. This is very similar to the results of our calculations on the protonation of excited formaldehyde.²¹

Again the positive E_{es} is well correlated with the positive E_H for these states in various BV-C and PV-C

(21) K. Morokuma, 27th Symposium on Molecular Structure and Spectroscopy, Columbus, Ohio, June 1972.

geometries. The ground and $\pi-\pi^*$ excited states which have a negative E_{es} are actually repulsive in these models. Further decomposition for $E_{pr} + E_{ct}$ into E_{pr} and E_{ct} suggests that it is E_{ct} that cancels with E_{ex} for those models giving a positive E_H . For BV models one finds a small negative E_{pr} for excited states, which may be attributed to higher order perturbation terms.

E. 1:2 Complex $H_2CO \cdots 2H_2O$. It is more likely that a carbonyl compound in the ground state is hydrated by two rather than one water molecule in the aqueous solution. A calculation in a previous paper¹ supported this trimer model. The model used is the same as the planar horizontal model PH 2 ($\theta = 60^\circ$, $R_{OH} = 1.9463 \text{ \AA}$, near the equilibrium) for the $H_2CO \cdots H_2O$ dimer, except that another H_2O is added to H_2CO at the symmetric position.

Here for the same trimer hydrogen-bond energy, transition energy and the charge transfer are calculated for various excited states. Results are given in Table X together with the PH 2 model dimer results. A hydrogen-bond energy of 2.50, 1.06, and 2.64 kcal/mol is gained by the interaction with the second H_2O molecule for the ground, $\pi-\pi^*$ triplet, and $\pi-\pi^*$ singlet states, respectively. These are as large as 73, 48, and 75% of the first hydrogen-bond energy for each state.

Table VIII. Hydrogen-Bond Energy, Its Components (kcal/mol) and the Charge Transfer for PV-C and BV-C Models for $\alpha = 0^\circ$

Model no. (geometry)	State	E_H	E_{es}	E_{ex}	$E_{pr} + E_{ct}$	ΔQ
PV-C 1 ($R_{BH} = 2.3 \text{ \AA}$, $\alpha = 0^\circ$)	Ground	-1.4	-0.2	-6.0	4.7	0.0059
	$^3(n-\pi^*)$	0.5	1.6	-6.2	5.5	0.0123
	$^1(n-\pi^*)$	0.4	1.6	-6.6	5.4	0.0124
	$^3(\pi-\pi^*)$	-1.5	-0.5	-5.2	4.2	0.0051
	$^1(\sigma-\pi^*)$	0.1	1.3	-6.6	5.4	0.0118
PV-C 2 ($R_{BH} = 2.8 \text{ \AA}$, $\alpha = 0^\circ$)	Ground	-0.3	-0.2	-0.9	0.8	0.0012
	$^3(n-\pi^*)$	0.5	0.5	-1.0	1.0	0.0025
	$^1(n-\pi^*)$	0.4	0.5	-1.0	0.9	0.0025
	$^3(\pi-\pi^*)$	-0.5	-0.4	-0.8	0.7	0.0011
	$^1(\sigma-\pi^*)$	0.4	0.4	-1.0	1.0	0.0024
BV-C 1 ($R_{BH} = 3.1 \text{ \AA}$, $\alpha = 0^\circ$)	Ground	-0.1	-0.1	-0.3	0.3	0.0006
	$^3(n-\pi^*)$	0.5	0.5	-0.3	0.3	0.0010
	$^1(n-\pi^*)$	0.4	0.5	-0.3	0.2	0.0011
	$^3(\pi-\pi^*)$	-0.3	-0.3	-0.2	0.2	0.0005
	$^1(\sigma-\pi^*)$	0.6	0.5	-0.3	0.4	0.0010

Table IX. Hydrogen-Bond Energy, Its Components (kcal/mol) and the Charge Transfer for BV-C Models for $\alpha \neq 0^\circ$

Model no. (geometry)	State	E_H	E_{es}	E_{ex}	$E_{pr} + E_{ct}$ (E_{pr}, E_{ct})	ΔQ
BV-C 2 ($R_{BH} = 2.5 \text{ \AA}$, $\alpha = 15^\circ$)	Ground	-0.5	-0.3	-2.3	2.1 (0.1, 2.0)	0.0031
	$^3(n-\pi^*)$	1.6	2.0	-2.8	2.4 (-0.5, 2.9)	0.0076
	$^1(n-\pi^*)$	1.2	1.9	-2.7	2.0 (-0.8, 2.8)	0.0078
	$^3(\pi-\pi^*)$	-0.6	-0.2	-2.1	1.8 (-0.1, 1.8)	0.0037
	$^3(\sigma-\pi^*)$	1.3	1.6	-2.7	2.3 (-0.3, 2.6)	0.0073
BV-C 3 ($R_{BH} = 2.8 \text{ \AA}$, $\alpha = 15^\circ$)	Ground	-0.1	-0.2	-0.7	0.8	0.0012
	$^3(n-\pi^*)$	1.2	1.4	-0.9	0.7	0.0028
	$^1(n-\pi^*)$	1.0	1.4	-0.9	0.5	0.0029
	$^3(\pi-\pi^*)$	-0.2	-0.1	-0.7	0.6	0.0014
	$^1(\sigma-\pi^*)$	1.0	1.1	-0.8	0.7	0.0027
BV-C 4 ($R_{BH} = 3.1 \text{ \AA}$, $\alpha = 15^\circ$)	Ground	-0.1	-0.2	-0.2	0.3 (0.1, 0.2)	0.0004
	$^3(n-\pi^*)$	0.7	0.9	-0.3	0.1 (0.2, 0.4)	0.0010
	$^1(n-\pi^*)$	0.5	0.9	-0.3	-0.1 (-0.4, 0.3)	0.0010
	$^3(\pi-\pi^*)$	-0.2	-0.2	-0.2	0.2 (-0.0, 0.2)	0.0005
	$^1(\sigma-\pi^*)$	0.7	0.7	-0.3	0.3 (-0.1, 0.3)	0.0010
BV-C 5 ($R_{BH} = 3.1 \text{ \AA}$, $\alpha = 30^\circ$)	Ground	-0.2	-0.3	-0.3	0.3	0.0003
	$^3(n-\pi^*)$	0.8	1.1	-0.3	-0.0	0.0009
	$^1(n-\pi^*)$	0.5	1.1	-0.3	-0.3	0.0009
	$^3(\pi-\pi^*)$	-0.2	-0.2	-0.2	0.2	0.0005
	$^1(\sigma-\pi^*)$	0.6	0.7	-0.3	0.1	0.0008

The $n-\pi^*$ states of the trimer are unstabilized, relative to the corresponding states of the isolated molecules, and are more unstable than those of the dimer.

The hydrogen-bond energy $E_H(\text{WHF})$ of the trimer can be divided into the sum of pair interactions and the nonadditive three-body interaction term $V(\text{WFW})$ ²²

$$E_H(\text{WFW}) = 2E_H(\text{FW}) + V(\text{W-W}) + V(\text{WFW})$$

where $E_H(\text{FW})$ is the hydrogen-bond energy of the dimer at this geometry when the second H_2O molecule is removed, and $V(\text{W-W})$ is the interaction energy of two H_2O molecules at this geometry in the absence of H_2CO . $V(\text{W-W})$ is -0.85 kcal/mol in this model. The calculated nonadditive three-body interaction

energy $V(\text{WFW})$ is shown in Table X. The nonadditive energy for all the states is smaller than that obtained for the water trimer with a large basis set.²² Consistent with the small nonadditive interaction, the amount of charge transfer, ΔQ , and the shift of the transition energy for the trimer are almost twice those for the dimer.

The calculated blue shift of the $n-\pi^*$ singlet transition 0.264 eV (2130 cm^{-1}) for the trimer is in good agreement with experiments that the blue shift in water of the acetone $(\text{CH}_3)_2\text{CO}$ $n-\pi^*$ singlet transition is about 1900 cm^{-1} .⁵

III. Basis Set Dependency of Hydrogen-Bond Energy and Its Components.

In the preceding section, we have used the minimal STO basis set. It is known that the hydrogen-bond energy in the *ab initio* calculation depends on the

(22) D. Hankins, J. W. Moskowitz, and F. H. Stillinger, *J. Chem. Phys.*, **53**, 4544 (1970).

Table X. Comparison between $\text{H}_2\text{CO}\cdots\text{H}_2\text{O}^a$ and $\text{H}_2\text{CO}\cdots 2\text{H}_2\text{O}^b$

State	Hydrogen-bond energy, kcal/mol			Charge transfer ΔQ		Vertical transition energy and shift in parentheses, eV	
	$\text{H}_2\text{CO}\cdots\text{H}_2\text{O}$ $E_{\text{H}}(\text{FW})$	$\text{H}_2\text{CO}\cdots 2\text{H}_2\text{O}$ $E_{\text{H}}(\text{WFW})$	$V(\text{WFW})$	$\text{H}_2\text{CO}\cdots\text{H}_2\text{O}$	$\text{H}_2\text{CO}\cdots 2\text{H}_2\text{O}$	$\text{H}_2\text{CO}\cdots\text{H}_2\text{O}$	$\text{H}_2\text{CO}\cdots 2\text{H}_2\text{O}$
Ground	3.39	5.88	-0.05	0.0197	0.0386		
$^3(n-\pi^*)$	-0.68	-2.11	0.10	0.0113	0.0212	3.28 (0.17)	3.45 (0.34)
$^1(n-\pi^*)$	0.23	-0.29	0.10	0.0108	0.0202	4.35 (0.13)	4.48 (0.26)
$^3(\pi-\pi^*)$	2.22	3.28	-0.31	0.0196	0.0386	4.10 (0.05)	4.16 (0.11)
$^1(\sigma-\pi^*)$	0.89	1.15	0.22	0.0093	0.0167	9.45 (0.10)	9.55 (0.20)
$^1(\pi-\pi^*)$	3.50	6.14	-0.01	0.0196	0.0384	15.11 (-0.02)	15.10 (-0.03)

^a Geometry of $\text{H}_2\text{CO}\cdots\text{H}_2\text{O}$: PH 2 ($\theta = 60^\circ$, $R_{\text{OH}} = 1.9463 \text{ \AA}$). ^b Geometry of $\text{H}_2\text{CO}_3\cdots 2\text{H}_2\text{O}$: add to the above $\text{H}_2\text{CO}\cdots\text{H}_2\text{O}$ another water at the symmetry position.

basis set.³ An extensive comparison has been made for the hydrogen-bond energy in the water dimer.²³

To examine the basis set dependency of the ground and excited state hydrogen-bond energies and their components, we have carried out calculations for $\text{H}_2\text{CO}\cdots\text{H}_2\text{O}$ with various Gaussian basis sets at the geometry found to be most stable in the ground state with the minimal STO basis set¹ (PH model with $R_{\text{OH}} = 1.89 \text{ \AA}$ and $\theta = 63.9^\circ$). Basis sets used are STO-3G¹⁰ (abbreviated as 3G), STO-3G augmented with a set of diffuse p orbitals (called 3G+p), 4-31G¹¹ (abbreviated as 431), and 4-31G augmented with a set of diffuse p orbitals²⁴ (called 431+p).

The hydrogen-bond energy and its components are shown in Table XI and Figure 7. In Table XI calculated dipole moments are also shown for H_2CO and H_2O . Experimental values are for the ground state of H_2O (1.86 D), for the ground state of H_2CO (2.34 D), and for the $^1(n-\pi^*)$ excited state (1.56 D)²⁵ but the last one cannot be compared directly with the values in the Table XI because they are calculated for the ground state geometry. For both molecules, the ground state dipole moment is underestimated by the STO-3G set, whereas it is overestimated by the other sets studied.

A glance at Figure 7 reveals that despite recognizable basis set dependencies of the hydrogen-bond energy and its components, the gross characteristic of ground and excited states is rather independent of the basis sets. The hydrogen-bond energy E_{H} is the largest in the ground state, smaller in $\pi-\pi^*$ states, and the smallest or even negative in $n-\pi^*$ states. This overall trend is mainly controlled by the electrostatic energy E_{es} , which also decreases in the same order. The order of the calculated dipole moment of H_2CO ($\mu_{\text{ground}} > \mu_{n-\pi^*} > \mu_{\pi-\pi^*}$) obviously determines this term. The exchange repulsion is only slightly state dependent. The $n-\pi^*$ states have a smaller repulsion, because in these states a lone pair n electron which can overlap strongly with the H_2O electron cloud is transferred into the π^* orbital. For the same reason the charge transfer or delocalization energy E_{ct} is smaller for the $n-\pi^*$ states. The singlet state has a larger polarization-resonance energy E_{pr} than the corresponding triplet state. As discussed before the difference is very roughly a measure of the resonance contribution. The singlet and triplet $n-\pi^*$ states have E_{pr} larger than the ground state, probably due to the increased polarizability upon excitation.

Now we will examine details of the basis set dependency of the hydrogen-bond energy and its components.

(23) J. E. Del Bene and J. A. Pople, *J. Chem. Phys.*, **56**, 3605 (1973).

(24) J. L. Whitten, *J. Chem. Phys.*, **56**, 5458 (1972).

(25) D. E. Freeman and W. Klemperer, *J. Chem. Phys.*, **45**, 52 (1966).

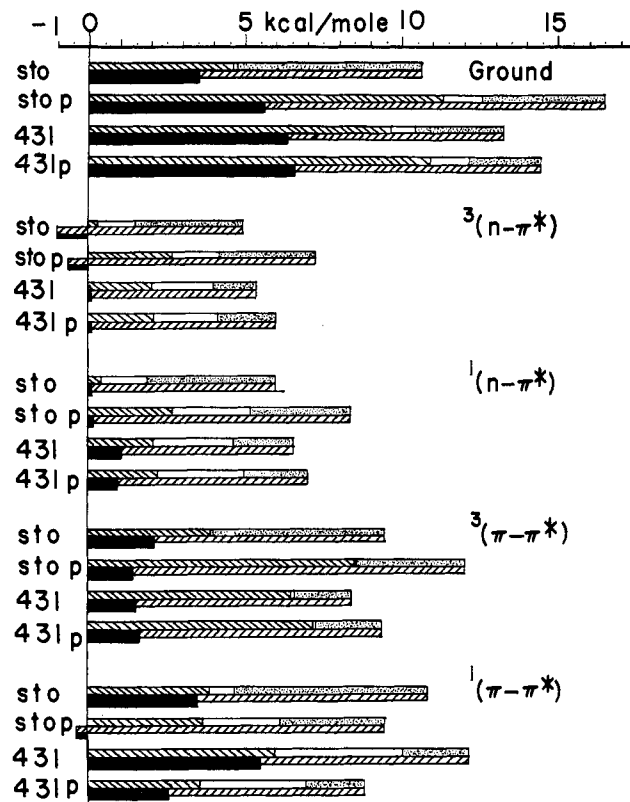


Figure 7. Hydrogen-bond energy and its components with various basis sets for the PH geometry at $R_{\text{OH}} = 1.89 \text{ \AA}$ and $\theta = 63.9^\circ$: (■) E_{H} ; (⊗) E_{es} ; (□) E_{pr} ; (⊞) E_{ex} ; and (⊘) E_{ct} .

The STO-3G set underestimates the dipole moments of the ground state molecules, whereas the other sets we used overestimate them. As the result, the electrostatic energy E_{es} whose leading term in the expansion in terms of the intermolecular distance r is $\mu_{\text{H}_2\text{CO}}\mu_{\text{H}_2\text{O}}/r^3$ is smaller in the STO-3G set than in other sets. Truth must lie between the two limits. A detailed comparison of E_{es} with the dipole moments μ in Table XI shows the E_{es} is not simply proportional to $\mu_{\text{H}_2\text{CO}}\mu_{\text{H}_2\text{O}}$, because at this intermolecular distance ($R_{\text{OH}} = 1.89 \text{ \AA}$), which is comparable to the size of molecules, the simple point dipole interpretation breaks down. The exchange repulsion E_{ex} is insensitive to the basis set. As the result, one sees that $E_{\text{es}} + E_{\text{ex}}$, which is $-(E_3 - E_0)$, is negative for the STO-3G set but is positive for the other sets.

The STO yields the largest charge-transfer energy, E_{ct} , which appears to be compensating the smallest electrostatic energy. The increase in E_{ct} in the STO-3G set compared with the other sets is not as large as the

Table XI. Hydrogen-Bond Energy, Its Components (kcal/mol) and Dipole Moment (μ , Debye)^a for Ground and Excited States with Various Basis Sets

State	Basis set	$\mu_{\text{H}_2\text{CO}}$	E_{H}	E_{es}	E_{ex}	E_{pr}	E_{ct}	ΔQ
Ground	3G	1.53	3.4	4.6	-7.3	0.1	5.9	0.027
	3G+p	3.08	5.6	11.4	-10.9	1.2	3.9	0.047
	431	3.01	6.3	9.7	-6.9	0.8	2.8	0.031
	431+p	3.18	6.6	10.8	-7.9	1.4	2.3	0.010
³ (n- π^*)	3G	0.48	-1.0	0.3	-5.9	1.2	3.4	0.015
	3G+p	0.68	-0.6	2.7	-7.9	1.5	3.0	0.042
	431	0.84	0.1	2.0	-5.4	2.0	1.4	0.019
	431+p	0.87	0.1	2.2	-5.9	2.0	1.8	0.003
¹ (n- π^*)	3G	0.38	0.1	0.4	-6.0	1.5	4.1	0.014
	3G+p	0.68	0.1	2.7	-8.3	2.5	3.2	0.041
	431	0.91	1.0	2.1	-5.5	2.6	1.9	0.018
	431+p	0.89	0.9	2.2	-6.1	2.8	2.0	0.002
³ (π - π^*)	3G	0.46	2.1	3.9	-7.3	0.0	5.5	0.027
	3G+p	1.14	1.4	8.5	-10.6	-0.1	3.7	0.047
	431	1.10	1.5	6.5	-6.9	0.1	1.8	0.030
	431+p	1.13	1.7	7.2	-7.7	0.0	2.1	0.010
¹ (π - π^*)	3G	0.80	3.6	3.9	-7.3	0.8	6.2	0.027
	3G+p	1.22	-0.4	3.6	-9.9	2.6	3.3	0.037
	431	0.33	5.5	6.0	-6.7	4.0	2.2	0.028
	431+p	0.47	2.5	3.6	-7.3	4.4	1.8	0.001

^a Dipole moment of the ground state H₂O: 3G, 1.71 D; 3G+p, 2.35 D; 431, 2.67 D; 431+p, 2.79 D.

decrease in E_{es} , so that the STO-3G set gives the smallest hydrogen-bond energy.

In connection with the large charge-transfer energy in STO minimal and STO-3G sets, Johansson, Kollman, and Rothenberg²⁶ discussed the "extra" dimer stabilization in STO-3G and showed that it arose mainly from an improvement in the representation of the 1s core orbital due to the additional basis set on the other molecule.

For the π - π^* singlet state the difference of the basis set should make a large difference in the nature of the π^* orbital. Despite all the changes of the π^* orbitals, no basis set can predict the red shift of the π - π^* singlet transition commonly observed experimentally among ketones and aldehydes upon hydrogen bonding (STO-3G gives a marginal red shift). We have also carried out calculations with STO-3G+p and 431G+p sets using very diffuse p orbitals (exponent 0.02 for the carbon and 0.05 for the oxygen), which gives an even larger blue shift of the π - π^* singlet state. Considering the fact that experimental shift values are mostly for conjugated ketones and aldehydes rather than simple ketones and aldehydes, we have carried out calculations for the acrolein-water system with the STO-3G and STO-3G + diffuse p sets, resulting in a red shift.²⁷ It does not appear that the dielectric effects of the bulk of the solvent can stabilize the less polar ¹(π - π^*) H₂CO more than the ground state H₂CO.

IV. Discussion and Conclusion.

In sections I, II, and III we have extended the energy decomposition scheme previously used for the ground state¹ to excited states. The definition of the components is made in terms of specific wave functions in the presence or absence of the interaction. Since no perturbation expansion is used, the components are well defined even when the interaction is relatively strong.

Kollman and Allen²⁸ broke up the total hydrogen-

bonding energy of HF and H₂O dimers into three contributions: (1) the electrostatic and charge cloud repulsion energies ΔE_{elect} , (2) the delocalization energy ΔE_{deloc} , and (3) the correlation energy ΔE_{corr} . The components ΔE_{elect} and ΔE_{deloc} correspond to $E_{\text{es}} + E_{\text{ex}}$ and $E_{\text{pr}} + E_{\text{ct}}$ in the present paper, respectively. Their results (in kilocalories per mole) of $E_{\text{es}} + E_{\text{ex}}$ and $E_{\text{pr}} + E_{\text{ct}}$ are 5.25 and 1.49, respectively, for (HF)₂ and 4.50 and 3.05 for (H₂O)₂. In the most stable geometry of H₂CO-H₂O ground state, our values are -2.7 and 6.0 (3G), 0.5 and 5.1 (3G+p), 2.8 and 3.6 (431), and 2.9 and 4.7 (431+p), respectively, as given in Table XI. Since the basis set used by Kollman and Allen is a split shell type, their values should be compared with ours with 431 and 431+p sets. Both components are positive in all three hydrogen-bond systems. $E_{\text{pr}} + E_{\text{ct}}$ is larger than $E_{\text{es}} + E_{\text{ex}}$ in H₂CO-H₂O, while the opposite is true in (H₂O)₂ and (HF)₂, indicating that H₂CO-H₂O is less electrostatic than the other two.

We have found that the hydrogen-bond energy and its components depend on the choice of the basis set. Despite this dependency, within each basis set the general characteristics of the ground and lower excited states are reasonably described by the energy decomposition pattern. This is encouraging in that, unless one is interested in the absolute values of components, one can use a relatively small basis set to compare various states.

After completing the detailed argument of section II, it is interesting to recognize that in an extremely qualitative sense the electrostatic energy E_{es} is often a good indicator of the hydrogen-bond energy E_{H} with a scaling factor which is less than unity. This conclusion might justify the simple electrostatic model recently reported by Bonaccorsi, Petrongolo, Scrocco, and Tomasi.²⁹ In general, E_{pr} is rather small, and $E_{\text{ct}} + E_{\text{pr}}$ tends to cancel with E_{ex} . This is probably because both E_{ct} and E_{ex} are related to the overlap of orbitals between the two molecules.

(26) A. Johansson, P. Kollman, and S. Rothenberg, *Theor. Chim. Acta*, **29**, 167 (1973).

(27) S. Iwata and K. Morokuma, submitted for publication.

(28) P. Kollman and L. C. Allen, *Theor. Chim. Acta*, **18**, 399 (1970).

(29) R. Bonaccorsi, C. Petrongolo, E. Scrocco, and J. Tomasi, *Theor. Chim. Acta*, **20**, 331 (1971).

Acknowledgment. This research is supported in part by the National Science Foundation (Grant GP-33998X) and by the Center for Naval Analyses of the University of Rochester. S. I. is on leave from the Institute of Physical and Chemical Research, Wako, Saitama, Japan.

Appendix

Calculation of Energy E_3^i for Excited States Based on the Antisymmetric Product of Two Isolated Molecular Wave Functions. The single configuration wave function for an excited state corresponding to an electron excitation from MO α to MO μ ($\phi_\alpha \rightarrow \phi_\mu$) is described as

$${}^1, {}^3\Phi = (1/\sqrt{2})[\{\phi_1(1)\bar{\phi}_1(2)\dots\phi_{n-1}(2n-3)\bar{\phi}_{n-1}(2n-2) \times \phi_\alpha(2n-1)\bar{\phi}_\mu(2n)\} \pm \{\phi_1(1)\bar{\phi}_1(2)\dots\phi_{n-1}(2n-3) \times \bar{\phi}_{n-1}(2n-2)\phi_\mu(2n-1)\bar{\phi}_\alpha(2n)\}] \equiv (1/\sqrt{2})[\{\dots\alpha\bar{\mu}\} \pm \{\dots\mu\bar{\alpha}\}] \quad (\text{A-1})$$

where $\{ \}$ is a Slater determinant and $\phi_1, \dots, \phi_{n-1}$ are assumed not to include ϕ_α or ϕ_μ . The plus and minus signs correspond to the singlet and triplet, respectively.

We assume MO's are normalized but not orthogonal. The nonorthogonal form is rather inconvenient for the energy calculation. By any orthogonalization technique such as the Schmidt method, one can mutually orthogonalize (and renormalize) doubly occupied MO's ϕ_1 to ϕ_{n-1} without changing the total wave function ${}^1, {}^3\Phi$ except for the unimportant normalization constant. Let us assume this has been done. The orthonormalization of ϕ_α to the now orthonormal $\phi_1, \phi_2, \dots, \phi_{n-1}$ does not change the total wave function. The orthonormalization of ϕ_μ to $\phi_1, \phi_2, \dots, \phi_{n-1}$

does not change the total wave function either. Let us assume that these orthonormalizations have been completed and that $\phi_1, \phi_2, \dots, \phi_{n-1}, \phi_\alpha$, and ϕ_μ describe resultant MO's. Now let us orthonormalize the new ϕ_μ to the new ϕ_α by using

$$\phi_\mu' = (\phi_\mu - S_{\alpha\mu}\phi_\alpha)/(1 - S_{\alpha\mu}^2)^{1/2} \quad (\text{A-2})$$

where $S_{\alpha\mu}$ is the overlap integral between ϕ_μ and ϕ_α . The total wave function is then

$${}^1, {}^3\Phi = \sqrt{2}S_{\alpha\mu}\{\dots\alpha\bar{\alpha}\} + (1/\sqrt{2}) \times (1 - S_{\alpha\mu}^2)^{1/2}[\{\dots\alpha\bar{\mu}'\} \pm \{\dots\mu'\bar{\alpha}\}] \quad (\text{A-3})$$

which is not normalized. The energy associated with this is written as

$${}^1, {}^3E = [\langle \dots\alpha\bar{\alpha} | S_{\alpha\mu} \{ E(\dots\alpha\bar{\alpha}) S_{\alpha\mu} + 2(1 - S_{\alpha\mu}^2)^{1/2} \times \langle \dots\alpha\bar{\alpha} | H | \dots\alpha\bar{\mu}' \rangle \} + (1 - S_{\alpha\mu}^2) \{ E(\dots\alpha\bar{\mu}') \pm K_{\alpha\mu}' \} / (1 + S_{\alpha\mu}^2)] \quad (\text{A-4})$$

In the EHP method the common MO's can be used for both the ground and excited states.⁷ Therefore, $E(\dots\alpha\bar{\alpha})$ is the ground state energy E^G . $E(\dots\alpha\bar{\mu}') \pm K_{\alpha\mu}'$ can be replaced by the excitation energy ${}^1, {}^3\Delta E(\alpha \rightarrow \mu')$ plus the ground state energy E^G . $\langle \dots\alpha\bar{\alpha} | H | \dots\alpha\bar{\mu}' \rangle$ is replaced by $\sqrt{2}F_{\alpha\mu}'$, where $F_{\alpha\mu}'$ is the matrix element of the Hartree-Fock operator between MO α and μ' .

Thus the energies for the singlet and triplet states ${}^1, {}^3\Phi(\alpha \rightarrow \mu)$ are, respectively

$${}^3E = E^G + {}^3\Delta E(\alpha \rightarrow \mu') \quad (\text{A-5})$$

$${}^1E = E^G + [(1 - S_{\alpha\mu}^2) {}^1\Delta E(\alpha \rightarrow \mu') + 2\sqrt{2}S_{\alpha\mu}(1 - S_{\alpha\mu}^2)^{1/2}F_{\alpha\mu}'] / (1 + S_{\alpha\mu}^2) \quad (\text{A-6})$$

The above described procedure was followed for the actual calculation of the energy associated with Φ_0^F ; Φ_0^W .

Semiempirical Molecular Orbital Calculations and Molecular Energies. A New Formula for the β Parameter

Patrick Coffey*¹ and Karl Jug

Contribution from the Department of Chemistry, St. Louis University, St. Louis, Missouri 63156. Received April 23, 1973

Abstract: A new expression for the core Hamiltonian integral H_{ab} over symmetrically orthogonalized orbitals is derived for semiempirical MO methods, based on the commutator equation $[\mathbf{r}, h] = \mathbf{p}$. Implementation of this formula leads to a theoretically satisfactory improvement for the INDO method. The formula is parameterized so as to duplicate the binding energies of homonuclear diatomic molecules. Calculations on a large number of first row diatomics and triatomics show a marked improvement for bond energies and force constants and even some improvement of the good dipole moments and bond distances of the original INDO method.

Despite recent advances in computer technology, rigorous solution of the Roothaan-SCF equations is still not generally feasible for polyatomic molecules. The principal problem in *ab initio* calculations is the

(1) Department of Chemistry, Vanderbilt University, Nashville, Tenn. 37203.

large number of difficult integrals over basis functions that are required. The last decade has seen the introduction of a number of semiempirical all-valence electron SCF methods. Rather than actually evaluate all the integrals needed, these methods neglect many of the integrals altogether and take values for many of the